

Overview of the QPS Project

J.F. Lyon¹, D.A. Spong¹, B.E. Nelson¹, L.A. Berry¹, M.J. Cole¹, S.P. Hirshman¹,
D.J. Strickler¹, A.S. Ware², D.E. Williamson¹, P.J. Fogarty¹, P. Goranson¹,
D. Mikkelsen³, P.K. Mioduszewski¹, D.A. Monticello³

¹*Oak Ridge National Laboratory, P.O. Box 2009, Oak Ridge, TN 37831-8072, U.S.A.*

²*Department of Physics and Astronomy, University of Montana, Missoula, MT, 59812, U.S.A*

³*Princeton Plasma Physics Laboratory, P.O. Box 451, Princeton, NJ 08502, U.S.A*

Abstract. QPS is a very-low-aspect-ratio quasi-poloidally-symmetric stellarator with $\langle R \rangle = 0.95\text{--}1$ m, $\langle a \rangle = 0.3\text{--}0.4$ m, $\langle B_{\text{axis}} \rangle = 1$ T for a 1.5-s pulse, and $P_{\text{heating}} = 2\text{--}4$ MW. This paper describes the configuration flexibility of the QPS experiment now under design.

I. QPS EXPERIMENT AND MAGNETIC CONFIGURATION

The QPS compact stellarator [1] is being developed to test key features of quasi-poloidal symmetry at very low plasma aspect ratio, 1/2-1/4 that of existing stellarators: robustness of the MHD equilibrium, reduced neoclassical and anomalous transport, and MHD stability limits. Figure 1 shows a cutaway view of the QPS; the main device parameters are listed in Table 1. There are two field periods with 10 modular coils per period. Due to stellarator symmetry, there are only five different coil types, shown in different colors. In addition there are three sets of poloidal field coils, 12 toroidal field (TF) coils, and an Ohmic current solenoid. These coil sets allow plasma shape and position control and driving up to 50 kA of plasma current. Nine independent controls on the coil currents permit a wide range of magnetic configuration properties for physics scoping studies.

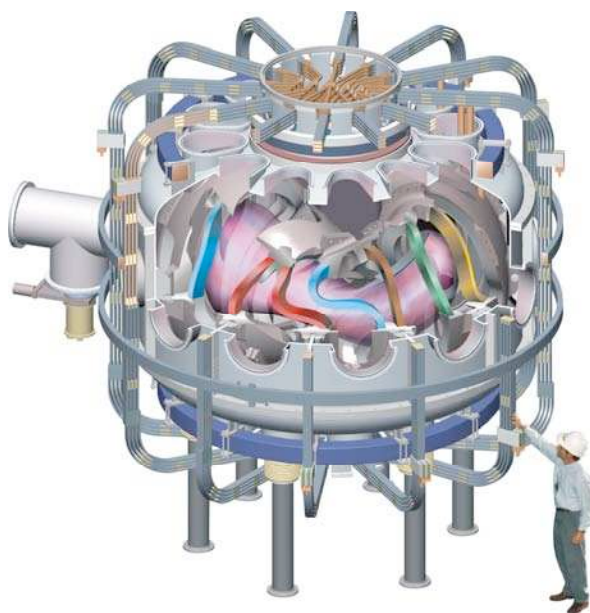


Table 1. QPS Device Parameters

Ave. major radius $\langle R \rangle$	0.9-1 m
Ave. plasma radius $\langle a \rangle$	0.3-4 m
Plasma aspect ratio	2.7
Plasma volume V_{plasma}	2-3 m ³
Central, edge rotational transform t_0, t_a	0.21, 0.32
Average field on axis from modular coils	$B_{\text{modular}} = 1$ T for 1.5 s
Auxiliary toroidal field	± 0.15 T
Ohmic current I_{plasma}	≤ 50 kA
ECH power	1.9 MW
ICRF heating power	1.5-3.5 MW

Fig. 1. Cutaway view of QPS.

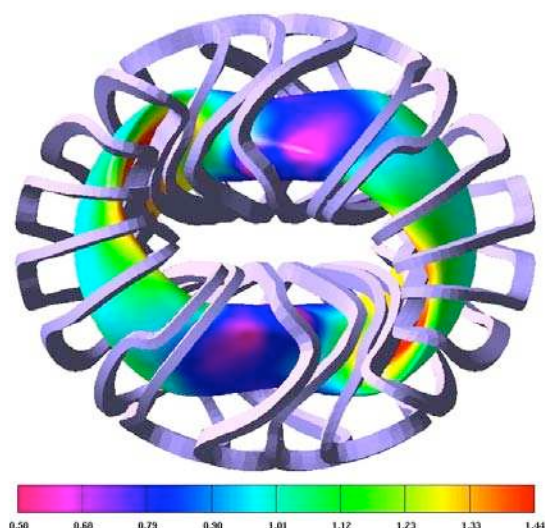


Fig. 2. Top (left) and side (above) views of the QPS plasma and the modular coils used to create it. The colors indicate contours of constant $|B|(T)$ on the last closed surface.

The shape of the QPS flux surfaces shown in Fig. 2 varies from bean-shaped at the high-field ends to D-shaped in the middle of the long sections. The resulting plasma elongation varies from 2 to 4.3. There is also a large helical excursion of the magnetic axis with $(R_{\max} - R_{\min})/\langle R \rangle = 0.53$ and $(z_{\max} - z_{\min})/\langle R \rangle = 0.45$. The dominant components in the magnetic field expansion are poloidally symmetric in "Boozer" flux coordinates, which leads to reduced neoclassical transport and decreased poloidal viscosity.

The good magnetic surfaces can be spoiled if magnetic islands occur due to field perturbations resonant at low-order rational values of the rotational transform $\iota = m/n$. Varying the degree of bootstrap and Ohmic currents allows avoiding

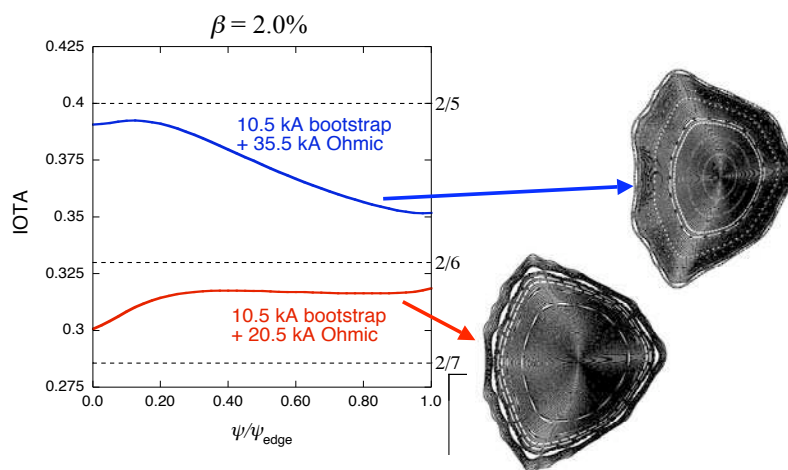


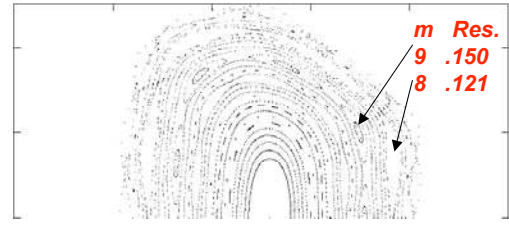
Fig. 3. Avoidance of low-order ι values and islands in QPS.

as shown in Fig. 3. Magnetic islands can also be minimized by varying the currents in the different coil sets subject to constraints on current limits and magnetic field. An optimization technique based on the Cary-Hanson method [2] is used to minimize the residue of targeted magnetic islands. Figure 4 illustrates the reduction in $m = 8$ and $m = 9$ magnetic islands in the vacuum fields using this technique. It is also possible to use external island correction coils as in W 7-AS and LHD.

II. MAGNETIC CONFIGURATION FLEXIBILITY

For no electric field in the low-collisionality limit, the neoclassical ripple-induced heat diffusivity is proportional to $\epsilon_{\text{eff}}^{3/2}$ where ϵ_{eff} is the effective ripple in a single helicity 1/v transport model that gives the same transport as a full 3-D calculation in this limit. QPS has an $\epsilon_{\text{eff}}^{3/2}$ similar to that in the W 7-X configuration, but at 1/4 the plasma aspect ratio. Figure 5 shows how changes in coil currents of $\pm 20\%$ allow a factor 12-36 variation in $\epsilon_{\text{eff}}^{3/2}$. Similarly, a factor 9 variation can be obtained in

QPS vacuum field - reference coil currents



Final state - minimum residues

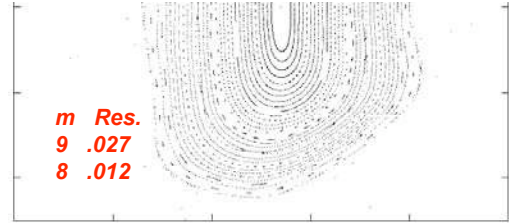


Fig. 4. Varying coil currents reduces magnetic islands in QPS.

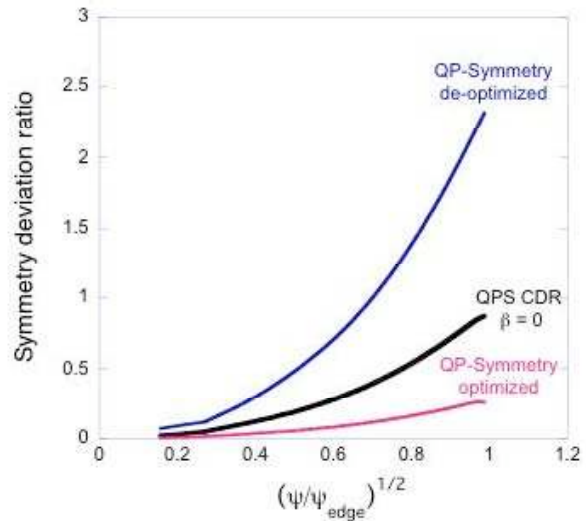
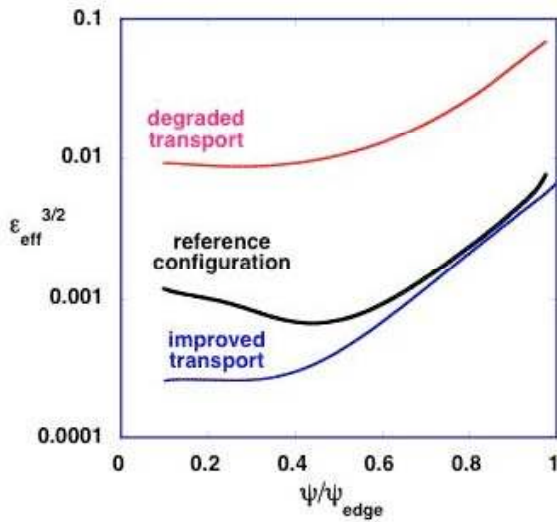


Fig. 5. Changes in the QPS coil currents permit varying degree of (a) neoclassical transport and (b) poloidal symmetry over a wide range.

the degree of poloidal symmetry as calculated by the ratio U/S of the magnetic energy in the non-symmetric modes (with poloidal mode number $m \neq 0$) to those that have poloidal symmetry (with $m = 0$). The fraction of the magnetic energy in non-poloidally symmetric field components is $<10\%$ in the plasma core ($r/a < 0.4$) and rises to $\sim 40\%$ at the plasma edge for the base (CDR) case. Here S excludes the flux surface average magnetic field ($m = 0, n = 0$) component. Including this term reduces the magnitude of the U/S ratio for the base (CDR) QPS configuration to 0.4% at $r/a = 0.4$ and 3% at the plasma edge.

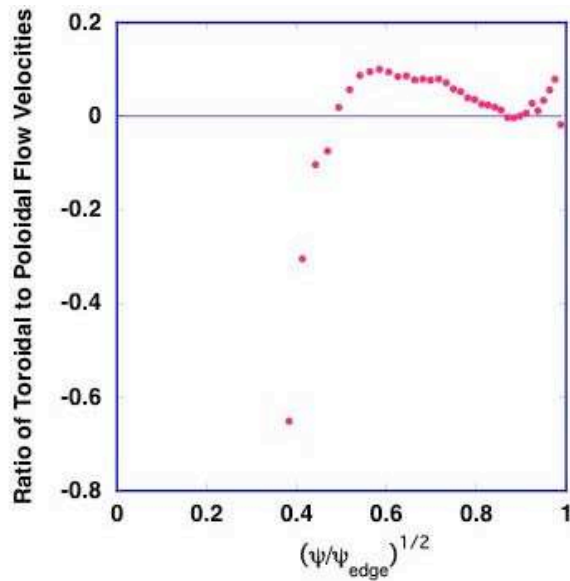


Fig. 6. Ratio of flow velocities for ICRF case.

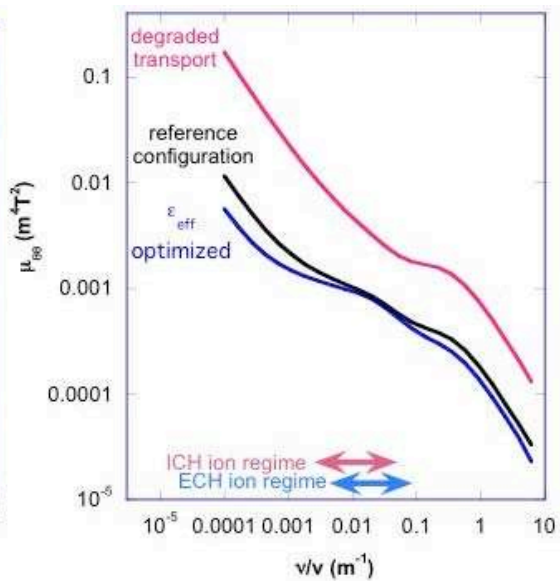


Fig. 7. Variation of poloidal viscosity.

The ambipolar electric field in QPS drives plasma rotation; the breakdown into poloidal and toroidal components is determined by the viscosity tensor. In QPS, poloidal flows are enhanced over toroidal flows. Large shear is present in both the electric field and the flow velocities, which should break up turbulent eddies and reduce anomalous transport. For typical ECH plasma parameters E_r and the poloidal velocity fall monotonically with radius. Root-jumping regions occur in the plasma due to a bifurcation in E_r . For typical ICRF-heated plasma parameters E_r and the flow velocities change sign and peak at $r/a \sim 0.6$ with no root jumping regions and the peak values are much reduced. However, poloidal flow dominates and toroidal flow is suppressed for both ECH and ICRF-heated plasmas, as discussed in Ref. 3. Figure 6 shows the ratio of toroidal to poloidal flow velocities for an ICRF-heated case. The toroidal flow velocity is less than 1/10 the poloidal flow velocity over more than half of the plasma radius; it reverses sign and becomes comparable with the poloidal velocity in the inner part of the plasma where the helical ripple is smaller. Changes in the coil currents allow a factor of 6–30 variation in the poloidal viscosity, (shown in Fig. 7), which permits studying the role of poloidal flows in suppressing turbulence.

Acknowledgments: This work was supported by the U.S. Dept. of Energy under contract DE-AC05-00OR22725 with UT-Battelle, LLC.

- [1] J. F. Lyon and the QPS team, "QPS, A Low Aspect Ratio Quasi-Poloidal Concept Exploration Experiment", <http://qps.fed.ornl.gov/>.
- [2] J. Cary, J. Hanson, *Phys. Fluids* **29**, 2464 (1986).
- [3] D. A. Spong et al., "Confinement Physics, Equilibrium Robustness, and Flexibility Studies of the Quasi-Poloidal Stellarator (QPS)", this conference.